ISSN 0010-5082, Combustion, Explosion, and Shock Waves, 2017, Vol. 53, No. 2, pp. 140–148. © Pleiades Publishing, Ltd., 2017.
Original Russian Text © I.S. Anufriev, A.M. Baklanov, O.V. Borovkova, M.S. Vigriyanov, V.V. Leshchevich, O.V. Sharypov.

Investigation of Soot Nanoparticles during Combustion of Liquid Hydrocarbons with Injection of a Superheated Steam Jet into the Reaction Zone

I. S. Anufriev[a], A. M. Baklanov[b], O. V. Borovkova[b,c], M. S. Vigriyanov[a], V. V. Leshchevich[d], and O. V. Sharypov[a,c]

UDC 62-643;662.613

Published in *Fizika Goreniya i Vzryva*, Vol. 53, No. 2, pp. 22–30, March–April, 2017.
Original article submitted December 1, 2015; revision submitted August 30, 2016.

Abstract: The characteristics of soot particles formed during combustion of liquid hydrocarbons in a laboratory model of an original burner with injection of a superheated steam jet into the reaction zone are experimentally studied. The concentration and size distribution of soot particles formed in the burner flame are measured by a diffusion aerosol spectrometer. It is shown that the majority of the primary particles have sizes ranging from 20 to 60 nm. The particle concentration in the external flame rapidly decreases with distance from the burner exit from 10^8 to $5 \cdot 10^6$ cm^{-3}. The images obtained by transmission electron microscopy demonstrate a chain-branched (fractal-like) structure of aggregates. The primary particles composing these aggregates have a union-like structure with the interplane distance between the layers smaller than 1 nm. Compact aggregates with sizes up to 500 nm are observed in cooled combustion products. The content of soot in combustion products is 35 mg/m^3, and the mean particle mass is $7 \cdot 10^{-12}$ mg. Results obtained in the combustion modes with injection of a superheated steam jet and with injection of an air jet are compared.

Keywords: burner, diesel fuel, steam jet, soot particles, diffusion aerosol spectrometer, transmission electron microscopy.

DOI: 10.1134/S0010508217020034

INTRODUCTION

Preliminary studies [1, 2] performed at the Kutateladze Institute of Thermophysics of the Siberian Branch of the Russian Academy of Sciences on original burners with powers of 10–50 kW [3] showed that combustion of liquid hydrocarbons becomes drastically intensified if a superheated (≈400°C) steam jet is injected into the reaction zone. In this case, there is practically no soot in the final combustion products. This method of fuel burning [4] may offer good prospects for utilization of low-quality fuels and hazardous industrial wastes with simultaneous generation of thermal energy. The development of burners operating in this mode requires investigations and scientific justification of new engineering solutions to ensure high energy efficiency and environmental friendliness of the technology, which potentially has numerous applications. For this purpose, it is necessary to take into account various features of complicated interrelated processes (heat and mass transfer, thermal decomposition of the fuel, heterogeneous processes, gasification, and ignition of fuel components) determining the rate of formation and composition of combustion products, the thermal effect, and other characteristics.

[a] Kutateladze Institute of Thermophysics, Siberian Branch, Russian Academy of Sciences, Novosibirsk, 630090 Russia; sharypov@itp.nsc.ru.
[b] Voevodskii Institute of Chemical Kinetics and Combustion, Siberian Branch, Russian Academy of Sciences, Novosibirsk, 630090 Russia.
[c] Novosibirsk State University, Novosibirsk, 630090 Russia.
[d] Luikov Institute of Heat and Mass Transfer, Belarus National Academy of Sciences, Minsk, 220072 Belarus.

This paper describes an experimental study of the characteristics of soot particles formed during combustion of the diesel fuel in a laboratory model of an original burner with injection of a superheated steam jet or an air jet.

EXPERIMENTAL FACILITIES AND MEASUREMENT TECHNIQUES

The study was performed in a laboratory model of an original burner with a power of 10 kW [1, 3, 5] (Fig. 1), which ensures fuel burning with the use of a superheated steam jet [4]. Heating of water and superheating of steam (≈400°C) entering the reaction zone through an injector were ensured due to reaction heat release. Natural inflow of air into the burner was provided. In this method of combustion, the evaporating fuel components are initially ignited in a situation with a lack of the oxidizer (oxygen contained in air); for this reason, the intermediate products contain a large amount of soot (region *4* in Fig. 1). Injection of a superheated steam jet into the reaction zone leads to gasification of the products of incomplete combustion of the fuel, intensification of the reaction, and carbon burnout. The generated syngas (consisting of CO and H_2) burns out in the flame, being mixed with oxygen from the ambient medium (region *6* in Fig. 1). The region of mixing of the products of incomplete combustion of the fuel and steam is located inside the burner (region *5* in Fig. 1). The position of region *5* is not changed if an air jet is injected instead of a steam jet.

The parameters of burner operation used in the study were the steam flow rate equal to 0.27 kg/h, the fuel flow rate equal to 0.6 kg/h, and the visible flame height equal to 120–140 mm.

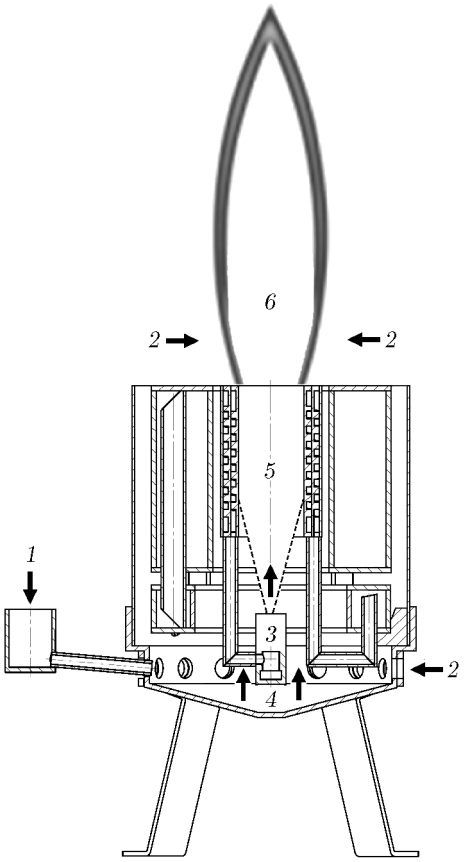

Fig. 1. Fuel combustion in the burner: (*1*) liquid fuel; (*2*) atmospheric air; (*3*) superheated steam; (*4*) region of ignition of the products of thermal decomposition of the fuel; (*5*) region of mixing of the products of incomplete combustion of the fuel and steam (region of gasification); (*6*) external flame (region of afterburning of the non-reacted components of the mixture in atmospheric air).

The mean concentration and the size distribution of soot particles in the external flame of the burner were determined by the diffusion aerosol spectrometer (DAS) developed at the Voevodskii Institute of Chemical Kinetics and Combustion of the Siberian Branch of the Russian Academy of Sciences [6–8]. The DAS consists of the following elements connected in series: diffusion battery (for separation of particles in accordance with their size), condensation particle magnifier (in which nanoparticles increase up to microscopic sizes owing to condensation of dibutyl phthalate), and photoelectric counter (for detection of enlarged particles). The operation principle of the diffusion battery is based on determining the diffusion coefficients of nanoparticles and reconstructing their size distribution from the known dependence of the diffusion coefficient of particles on their size. The diffusion coefficient of nanoparticles is determined from the penetration coefficient of aerosol particles passing through a porous medium or capillary tubes due to diffusion. A set of meshes mounted normal to a two-phase flow with particles is used as a porous medium. The developed mathematical model of diffusion-induced deposition of nanoparticles in such processes allows us to reconstruct their size distribution. For detecting and counting particles that passed through this section of the diffusion battery, they are directed to the condensation chamber where they enlarged to an optically detectable size and then proceed to the optical counter. The cycle of accumulation of raw data includes registration of concentrations of the aerosol consecutively sampled from each section of the diffusion battery. After that, computer processing of the set of the penetration coefficients is performed with the use of a special code for the DAS and the parti-

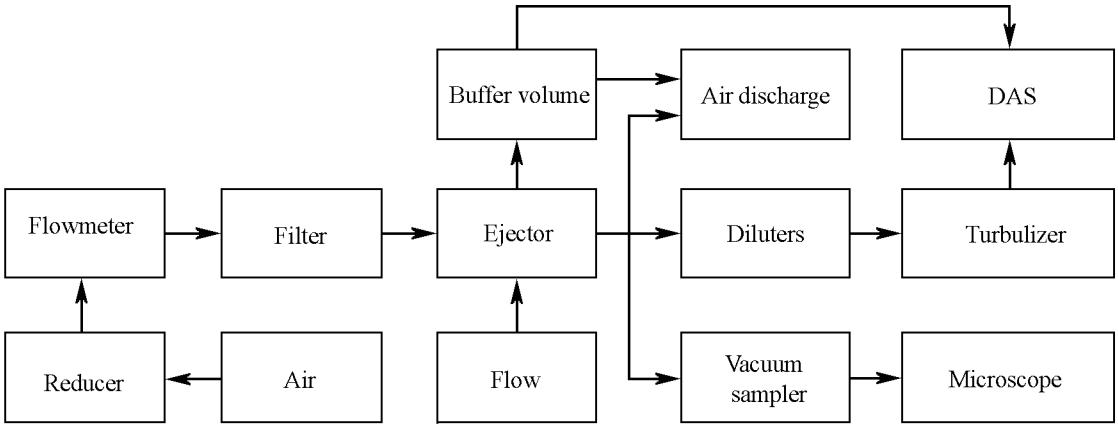

Fig. 2. Measurement scheme.

cle size distribution is determined. The basic characteristics of the instrument performance are the range of the measured particle diameters from 3 to 200 nm, the range of the measured concentrations without additional dilution smaller than $5 \cdot 10^5$ cm^{-3}, the volume flow rate of the analyzed aerosol equal to 1 liter/min, the time of one measurement of the particle size distribution equal to 3 min, the time of concentration measurement equal to 5 s, and the relative error of the analyzed aerosol of 10%. To measure higher concentrations (up to 10^9 cm^{-3}), two types of dilution are used: (1) dilution in the ejector chamber by means of mixing the aerosol flow with pure air; (2) separation of the flow with the aerosol into two parts, making one part pass through the aerosol filter, and mixing of both parts (with the use of the turbulizer). The instrument has been well approved in practice [9].

Sampling from the flame requires immediate dilution for cooling and "freezing" the processes of combustion and coagulation [10]. In the present study, sampling is performed through a special ejector. The ejector probe is a ceramic tube 95 mm long, with the inner and outer diameters being equal to 0.8 and 3 mm, respectively. For the flow rate through the probe of 1.2 liter/h, the flow velocity is 0.6 m/s, and the characteristic time of aerosol residence in the probe before dilution is 160 ms. The dilution coefficient of the ejector is determined by the volume flow rate of the incoming flow of pure air. The ejector was calibrated in the range of flow rates from 100 to 800 liters/h with the use of a film flowmeter. The dilution coefficient of the aerosol flow is affected by particle deposition in the probe. In the course of long-time sampling, the probe was regularly cleaned by means of purging with a large air flow.

The measurement technique was arranged in the following manner (Fig. 2). The compressed air flow from a pipeline (300 liters/h) passed through the reductor and variable-area flowmeter to the ejector. The typical dilution coefficient of the ejector was 100. With this level of dilution, the particle concentration was higher than the measurement limit of the instrument. Therefore, aerosol concentration diluters (by a factor of 20 and 10, depending on the measured concentration) were additionally placed behind the ejector, followed by the turbulizer for flow homogenization. In another variant, the flow from the ejector passed to the buffer volume during 1 min with a flow rate of 1 liter/min, from which a sample was then taken for the DAS analysis.

The samples for the electron microscope were taken by the vacuum sampler. Its advantage is its comparatively fast operation (sampling time 20 s), and its drawback is spectrum distortion because of predominant sampling of coarse particles. A traversing gear moved the ejector probe to different places of the flow. The particles were deposited onto a copper grid (3 mm in diameter, with the cell size of 40×40 μm) covered with a polyvinylformal film. Soot particles sampled at different points of the flame were photographed by the method of transmission electron microscopy (TEM) with two different microscopes (JEM-100SX and JEOL JEM-2010) to study the size and structure of aggregates being formed. In addition, the concentration of particles and their size distribution in combustion products cooled to room temperature in a flow-type calorimeter were measured [11]. Particles leaving the calorimeter were also sampled by the aerosol filter for mass analysis.

The same technique was used to perform measurements in the case of burning of the diesel fuel with injection of an air jet instead of steam into the reaction

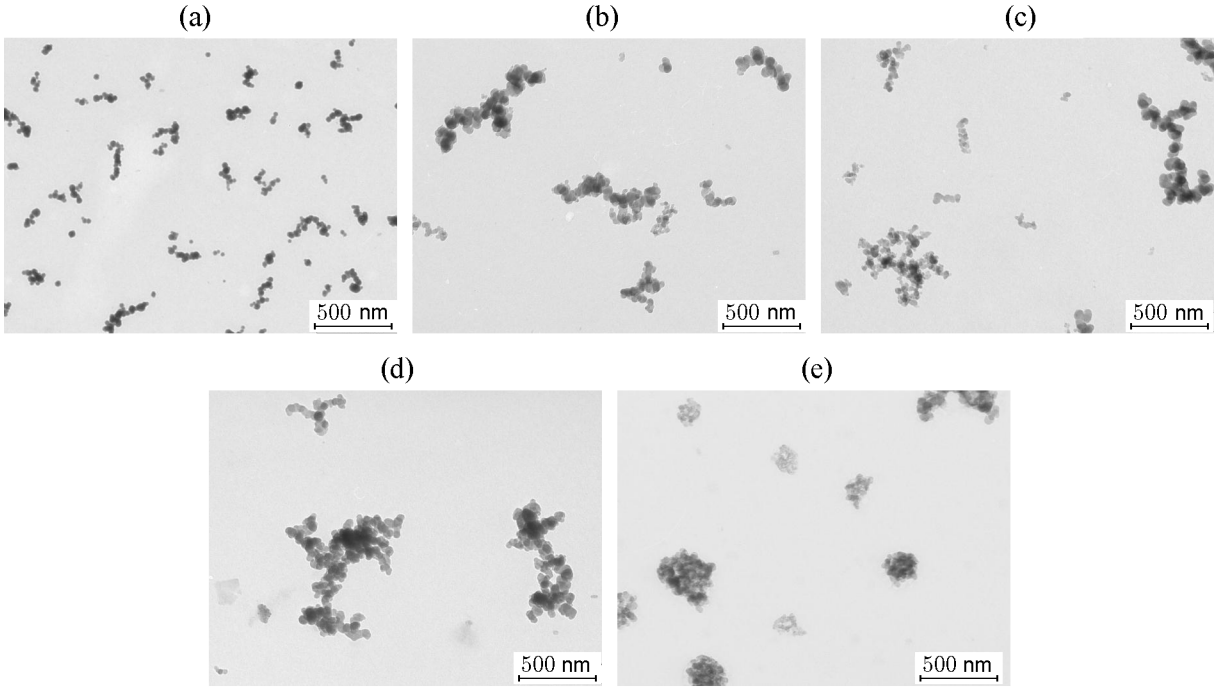

Fig. 3. TEM photographs (JEM-100SX microscope) of soot particles (regime with steam injection) sampled at different points of the flame: (a) $h = -20$ mm (in the region of gasification inside the burner); (b) $h = 0$ (at the burner exit, near the base of the external flame); (c) $h = 80$ mm (at the half-height of the visible flame); (d) $h = 120$ mm (in the upper part of the flame); (e) in cooled combustion products.

zone. Passing through the burner structure elements, air was heated to ≈330°C. The fuel flow rate in this regime was equal to the flow rate in the regime with steam injection. The Dwyer RMA-21-SSV flowmeter defined the flow rate of air equal to 5 liters/min. In this case, the external flame was visually equivalent to that in the combustion mode with steam injection.

As the flow was turbulent, it was impossible to perform local measurements of the soot particle size distribution because fairly intense mixing occurred during the time needed to measure one spectrum (4 min), and only the mean characteristics in the sampled flow region could be obtained.

RESULTS AND ANALYSIS

Figure 3 shows the TEM photographs of soot particles formed by burning the diesel fuel in the regime with steam injection. The samples were taken in the flame at the burner axis at different heights above the burner exit (h) and in combustion products cooled down to room temperature. The morphology of soot particles in the flame is a typical structure of fractal-like aggregates. The majority of these aggregates have a chain-branched structure consisting of spherical primary particles 20–60 nm in diameter. The characteristic size of the primary particles and the fractal dimension of aggregates equal to 1.8 ±0.1 in the external flame are in-

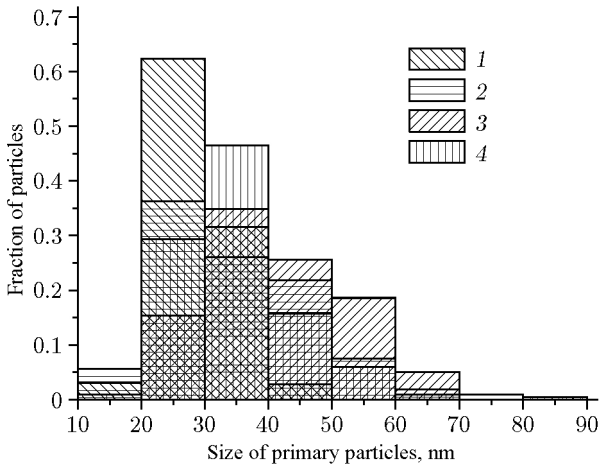

Fig. 4. Size distribution of the primary soot particles in aggregates formed in fuel burning with steam injection: (*1*) $h = -20$ mm (the mean particle size is 28 ± 5 nm); (*2*) $h = 0$ (34 ± 11 nm); (*3*) $h = 120$ mm (42 ± 11 nm); (*4*) cooled combustion products (35 ± 9 nm).

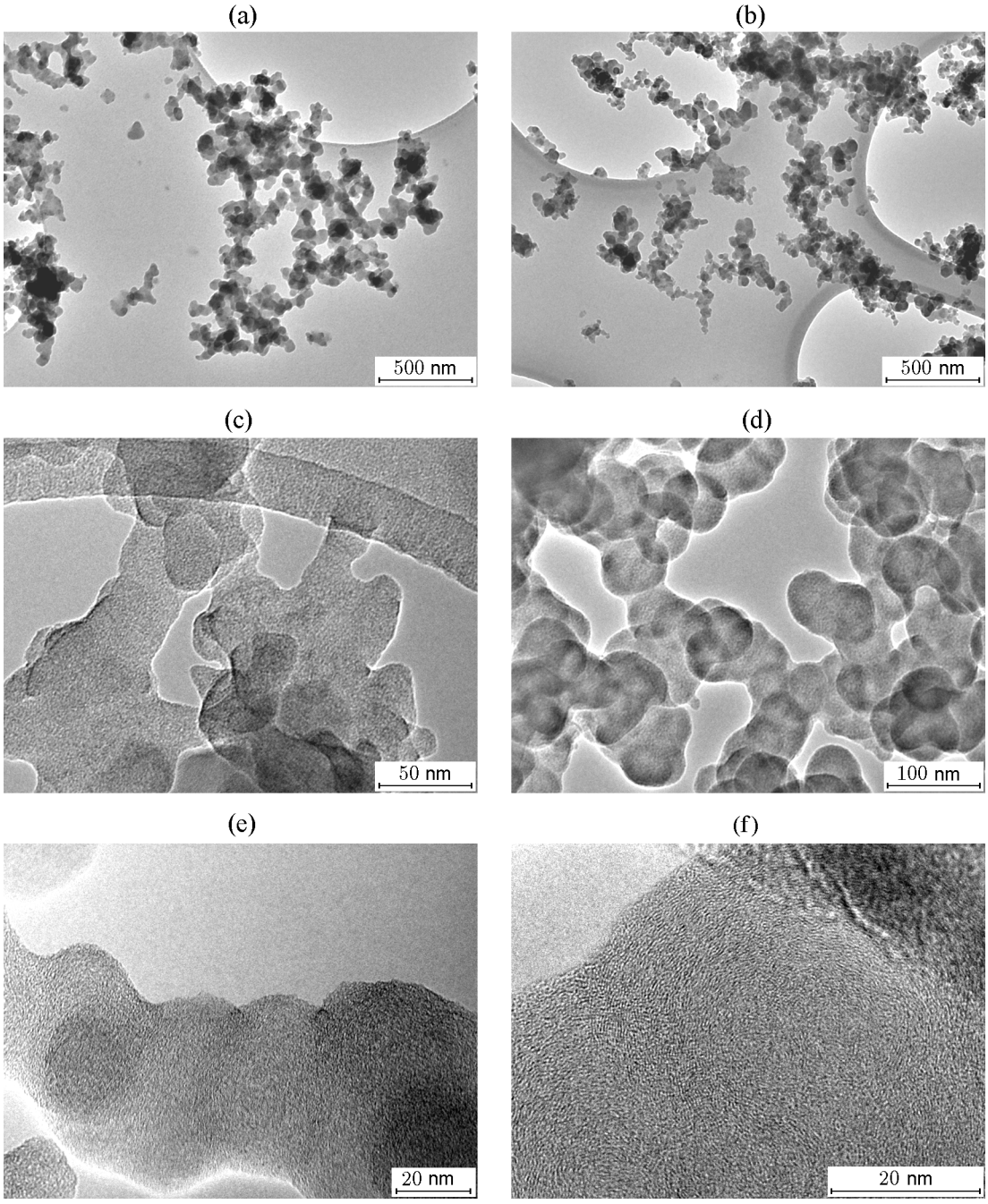

Fig. 5. TEM photographs (JEOL JEM-2010 microscope) of soot particles (regime with steam injection) sampled on the vertical axis inside the burner (a, c, and e) at $h = -20$ mm and at the burner exit (b, d, and f) at $h = 0$.

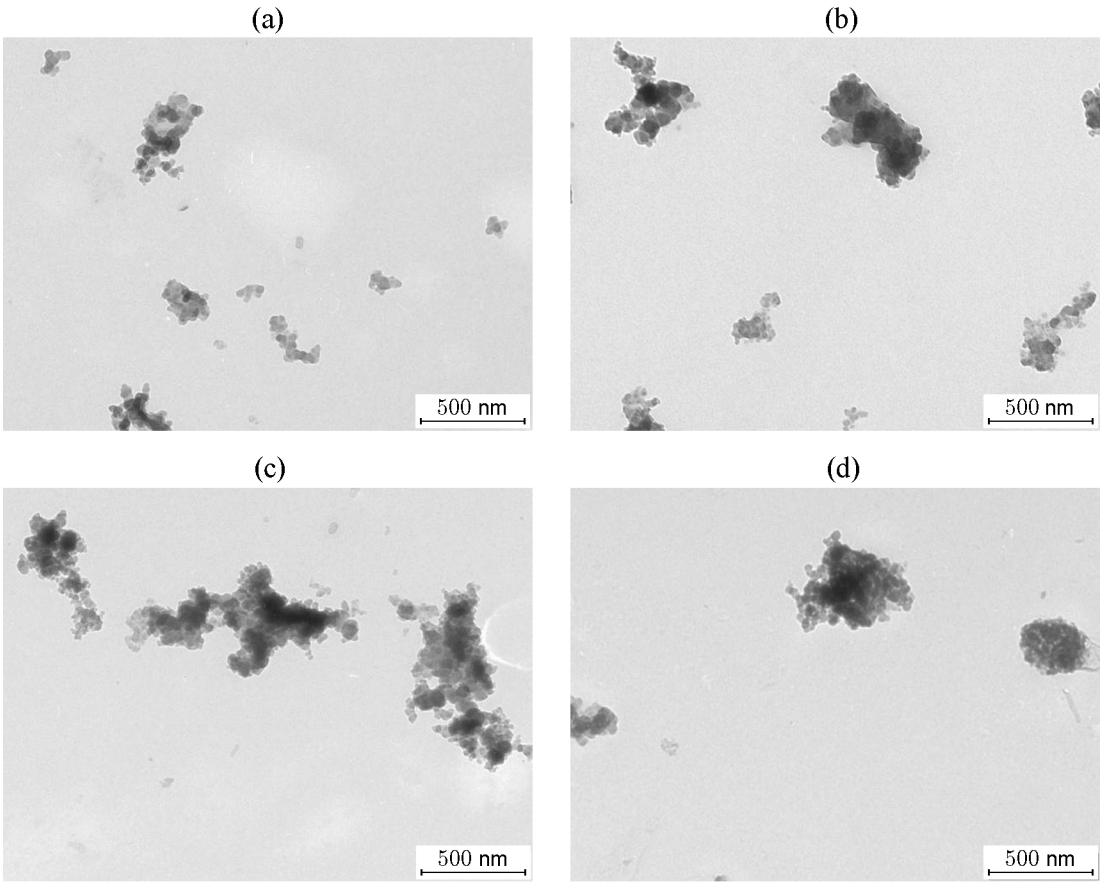

Fig. 6. TEM photographs (JEM-100SX microscope) of soot particles (regime with air injection) sampled at distances from the burner exit $h = -20$ (a), 80 (b), and 120 mm (c) and in cooled combustion products (d).

Size distribution of soot particles (see Fig. 7) during combustion in regimes with steam injection and air injection

Sampling point	Particle concentration (DAS), cm^{-3}		Mean particle size (DAS), nm		Mean geometric diameter, nm		Standard geometric deviation	
	steam	air	steam	air	steam	air	steam	air
On the flame axis, $h = 0$	$9 \cdot 10^7$	$4 \cdot 10^7$	39.4	78.0	44.5	122.9	1.3	1.9
On the flame axis, $h = 140$ mm	$8 \cdot 10^6$	$6 \cdot 10^6$	35.1	77.1	39.5	87.9	1.9	1.5
In cooled combustion products	$5 \cdot 10^6$	$4 \cdot 10^6$	58.7	79.3	65.9	98.8	1.7	1.2

dependent of h. The characteristic size of aggregates increases with increasing h. The size of the primary particles in the gasification region is appreciably smaller than in the external flame (Fig. 4). With a higher spatial resolution (Fig. 5), it is seen that an union-like structure is typical for the primary particles [12]. Concentric layers have an atomic thickness (Figs. 5e and 5f), contain multiple defects, and are arranged in a disordered manner relative to each other. The interplane distance between the layers is smaller than 1 nm.

Figure 6 shows the TEM photographs of the soot particles formed due to burning the diesel fuel with injection of air (instead of steam) into the reaction zone. The analysis of the TEM images shows that the aggre-

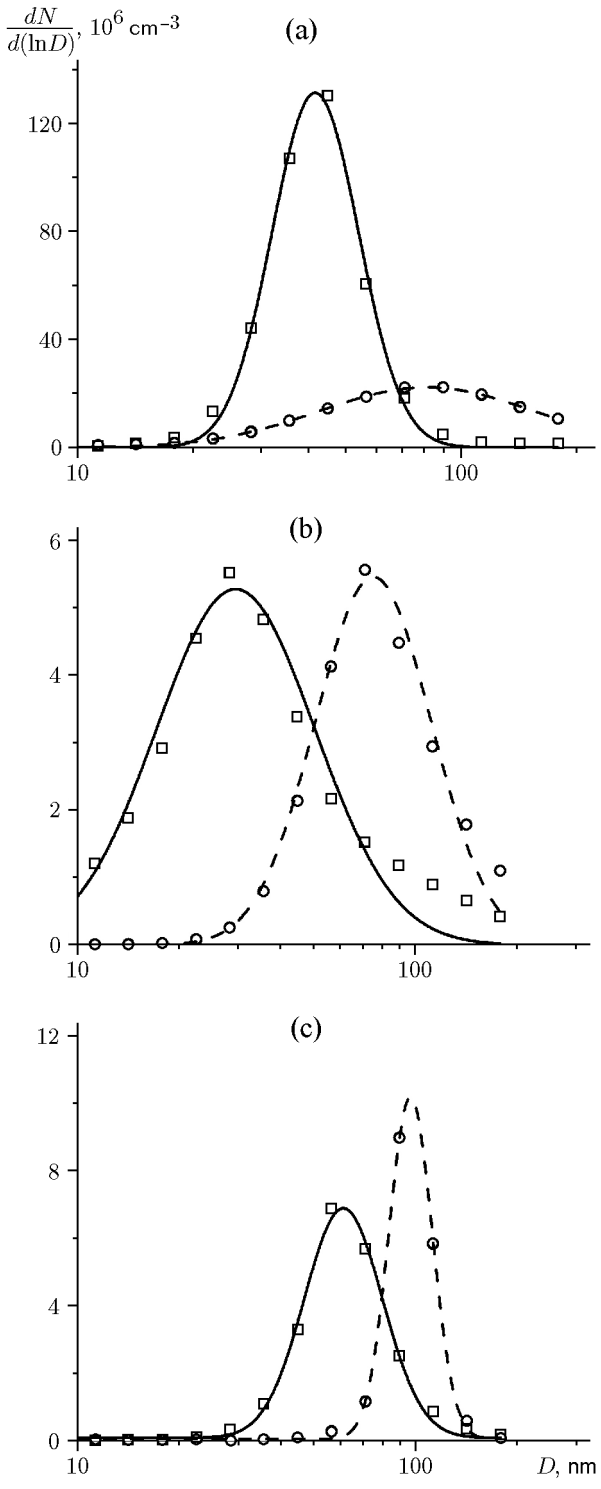

Fig. 7. Size distribution of soot particles formed in the regime of combustion with steam injection (squares and solid curve) and in the regime with air injection (circles and dashed curve) at sampling points $h = 0$ (a) and 140 mm (b) and in cooled combustion products (c) (the curves show the results of log-normal approximation).

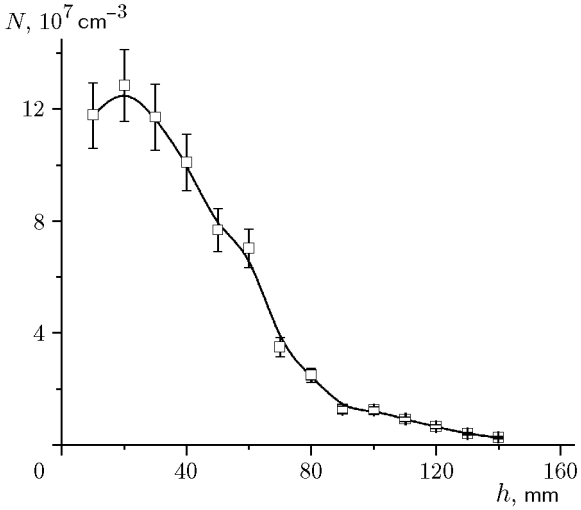

Fig. 8. Concentration distribution of soot particles along the vertical axis of the burner (regime of combustion with steam injection).

gates being formed also have a chain-branched structure, and the size of the primary particles is approximately identical to that in the regime with steam injection. However, in the regime with an air jet, the primary particles are more densely packed in the aggregates. In cooled combustion products (with a long lifetime), the branched aggregates become more compact, and their shapes approach spheres with a typical diameter of 400–500 nm (Fig. 6d). In the regime with a steam jet, compact aggregates of smaller sizes are formed (see the DAS spectra in Fig. 7 and the table). These observations are qualitatively consistent with the TEM results (see Fig. 3e).

Figure 7 shows the particle size distribution obtained by the DAS. In the regime of combustion with steam injection, the majority of particles at the burner exit ($h = 0$) have the size $D = 40 \pm 15$ nm, which corresponds to the characteristic size of the primary particles determined from the photographs in Figs. 3 and 5. This means that most of the total number of soot particles in the flow are primary non-aggregated particles. The fraction of these particles decreases in the downstream direction. The absence of individual primary particles in the photographs in Figs. 3, 5, and 6 is explained by the above-noted specific features of sampling for the electron microscope: low-inertia primary particles are entrained by the gas flow and only more massive particles (aggregates) become deposited on the film surface. In the regime of combustion with air injection (see Fig. 7), the spectrum of the particle size distribution is significantly wider and the most representative particle size is approximately twice greater.

The DAS was used to measure the soot particle concentrations in the external flame along the vertical axis of the burner with a spatial step of 10 mm (Fig. 8). It is seen that the concentration (N) of soot particles in the flame rapidly decreases from the maximum value of $\approx 10^8$ cm^{-3} with increasing distance from the burner exit and approaches the lower limit of $5 \cdot 10^6$ cm^{-3}. A similar dependence of the concentration of soot particles in combustion products is also typical for the regime of combustion with injection of compressed air instead of steam into the reaction zone (the qualitative results are summarized in the table).

Processing the TEM images, we obtained the size distribution of the primary particles in the aggregate and the mean arithmetic value (≈40 nm), which depends neither on the point of sampling in the external flame, nor on the combustion mode within the margins of the measurement error (see Fig. 4).

To perform the mass analysis of soot particles in cooled combustion products, we used a pump for sampling onto the aerosol filter at the place where the flow left the flow-type calorimeter. The flow rate was $Q = 6.0$ liters/min, and the sampling duration was 17 min. The mass of soot particles deposited during this time turned out to be $M = 3.5$ mg (0.2 mg/min), i.e., the soot content in combustion products is approximately 35 mg/m^3.

If the particle concentration in cooled combustion products is known ($N = 5 \cdot 10^6$ cm^{-3} as determined by the DAS), it is possible to use the formula $M = QmNt$ to estimate the mean particle mass: $m \approx 7 \cdot 10^{-12}$ mg. For the soot density of 2 g/cm^3 [7], the mean-mass diameter of soot particles is approximately 0.2 μm.

CONCLUSIONS

The results of studying the size distribution of soot particles with the use of a diffusion aerosol spectrometer show that the dominant particle size in the flow is 40 ± 15 nm. The concentration of soot particles in the burner flame reaches 10^8 cm^{-3}. The soot concentration rapidly decreases with distance from the flame base owing to mixing of the flow with ambient air and reaches $5 \cdot 10^6$ cm^{-3} in combustion products. Reduction of the particle concentration can be also assisted by particle coagulation (to a smaller extent).

The morphology of aggregates formed due to coagulation of the primary soot particles was analyzed by means of transmission electron microscopy. The aggregates in the flame have a chain-branched structure. In the combustion products, the aggregates have a more compact shape, and their typical size is 200–500 nm. The primary particles in these aggregates are characterized by a quasi-spherical shape (with a diameter of ≈40 nm) and an union-like structure with the interplane distance between the layers being smaller than 1 nm. The mean size of the images of the primary particles agrees well with the data of diffusion spectrometry.

The mass analysis shows that 1 m^3 of combustion products contains 35 mg of soot. Thus, for the diesel fuel flow rate of 600 g/h (515 g of carbon per hour) and the mean volume flow rate of the exhaust gas equal to 15 m^3/h in the experiment, the unburned carbon fraction is approximately 0.1%. The calculated value of the mean particle mass corresponds to the mean mass particle size of 0.2 μm, which is appreciably greater than the dominant size of the primary particles, i.e., the main mass of soot in combustion products is concentrated in aggregates.

A comparison of the results obtained in the combustion regimes with injection of superheated steam and air jets into the reaction zone shows that coagulation occurs in a different manner in these regimes despite an identical mean size of the primary soot particles. In the regime of combustion with air injection, the particle sizes are more scattered, and the representative particle size is almost twice greater than that in the regime of combustion with steam injection. Nevertheless, the concentration of soot particles in combustion products is approximately identical in both combustion modes.

This work was supported by the Russian Foundation for Basic Research [Grant Nos. 14-08-00177-a, 15-38-20558-mol_a_ved, and 15-58-04032-Bel_mol_a (BRFFI F15RM-044)], by the educational scholarship of the President of the Russian Federation for young researchers and post-graduate students (Grant No. SP-1410.2015.1), and by the Program of basic research of the Russian Academy of Sciences entitled "Basic Research of Combustion and Explosion Processes."

REFERENCES

1. S. V. Alekseenko, I. S. Anufriev, M. S. Vigriyanov, V. M. Dulin, E. P. Kopyev, and O. V. Sharypov, "Steam-Enhanced Regime for Liquid Hydrocarbons Combustion: Velocity Distribution in the Burner Flame," Teplofiz. Aeromekh. **21** (3), 411–414 (2014) [Thermophys. Aeromech. **21** (3), 393–396 (2014)].
2. S. V. Alekseenko, S. E. Pashchenko, and V. V. Salomatov, "Nanocluster Initiation of Combustion of Off-Grade Hydrocarbon Fuels," Inzh.-Fiz. Zh. **83** (4), 682–693 (2010) [J. Eng. Phys. Thermophys. **83** (4), 729–741 (2010)].
3. M. S. Vigriyanov, S. V. Alekseenko, I. S. Anufriev, and O. V. Sharypov, "Burner," RF Patent No. 2523591, Registered May 27, 2014, Published July 20, 2014, Bul. No. 20, Priority April 09, 2013.

4. M. S. Vigriyanov, M. S. Salomatov, and S. V. Alekseenko, "Method of Soot-Free Burning of Fuels," RF Patent No. 2219435, Applied February 11, 2002, Published December 20,2003.
5. I. S. Anufriev, E. P. Kopyev, and E. L. Loboda, "Study of Flame Characteristics during Liquid Hydrocarbons Combustion with Steam Gasification," in *Proc. of the 20th Int. Symp. on Atmospheric and Ocean Optics: Atmospheric Physics*, 929226 (November 25, 2014); DOI: 10.1117/12.2086623.
6. A. N. Ankilov, A. M. Baklanov, R. Mavliev, et al., "Comparison of the Novosibirsk Automated Diffusion Battery with the Vienna Electro Mobility Spectrometer," J. Aerosol Sci. **22**, S325–S328 (1991).
7. A. A. Onischuk, S. di Stasio, V. V. Karasev, et al., "Evolution of Structure and Charge of Soot Aggregates during and after Formation in a Propane/Air Diffusion Flame," J. Aerosol Sci. **34**, 383–403 (2003).
8. *Diffusion Aerosols Spectrimeter: Manual* (Aerosol Instruments, Novosibirsk, 2013) [in Russian].
9. E. O. Knutson, "History of Diffusion Batteries in Aerosol Measurements," Aerosol Sci. Technol. **31**, 83–128 (1999).
10. S. K. Friedlander, *Smoke, Dust and Haze. Fundamental of Aerosol Dynamics* (Oxford Univ. Press, New York, 2000).
11. S. V. Alekseenko, I. S. Anufriev, M. S. Vigriyanov, E. P. Kopyev, and O. V. Sharypov, "Characteristics of Diesel Fuel Combustion in a Burner with Injection of a Superheated Steam Jet," Fiz. Goreniya Vzryva **52** (3), 37–44 (2016) [Combust., Expl., Shock Waves **52** (3), 286–293 (2016)].
12. T. Ishiguro, Y. Takatori, and K. Akihama, "Microstructure of Diesel Soot Particles Probed by Electron Microscopy: First Observation of Inner Core and Outer Shell," Combust. Flame **108** (1/2), 231–234 (1997).